



OIST

OKINAWA INSTITUTE OF SCIENCE AND TECHNOLOGY GRADUATE UNIVERSITY
沖縄科学技術大学院大学


Proximity proteomics identifies cancer cell membrane cis molecular complex as a potential cancer target

Author	Norihiro Kotani, Arisa Yamaguchi, Tomoko Ohnishi, Ryusuke Kuwahara, Takanari Nakano, Yuka Nakano, Yui Ida, Takayuki Murakoshi, Koichi Honke
journal or publication title	Cancer Science
volume	110
number	8
page range	2607-2619
year	2019-06-22
Publisher	John Wiley & Sons Australia, Ltd on behalf of Japanese Cancer Association
Rights	(C) 2019 The Author(s).
Author's flag	publisher
URL	http://id.nii.ac.jp/1394/00001025/

doi: info:doi/10.1111/cas.14108

ORIGINAL ARTICLE

Proximity proteomics identifies cancer cell membrane *cis*-molecular complex as a potential cancer target

Norihiro Kotani¹  | Arisa Yamaguchi² | Tomoko Ohnishi² | Ryusuke Kuwahara³ |
Takanari Nakano¹ | Yuka Nakano¹ | Yui Ida¹ | Takayuki Murakoshi¹ | Koichi Honke²¹Department of Biochemistry, Saitama Medical University, Saitama, Japan²Department of Biochemistry, Kochi University Medical School, Kochi, Japan³Quantum Wave Microscopy Unit, Okinawa Institute of Science and Technology Graduate University (OIST), Okinawa, Japan**Correspondence**Norihiro Kotani: Department of Biochemistry, Saitama Medical University, 38 Morohongo, Moroyama-machi, Iruma-gun, Saitama 350-0495, Japan.
Email: kotani@saitama-med.ac.jp**Funding information**

Mizutani Foundation for Glycoscience; Japan Science and Technology Agency; Grants-in-aid for Scientific Research in Japan, Grant/Award Number: JP24590082, JP15K07941 and JP18K06663

Abstract

Cancer-specific antigens expressed in the cell membrane have been used as targets for several molecular targeted strategies in the last 20 years with remarkable success. To develop more effective cancer treatments, novel targets and strategies for targeted therapies are needed. Here, we examined the cancer cell membrane-resident “*cis*-bimolecular complex” as a possible cancer target (*cis*-bimolecular cancer target: BiCAT) using proximity proteomics, a technique that has attracted attention in the last 10 years. BiCAT were detected using a previously developed method termed the enzyme-mediated activation of radical source (EMARS), to label the components proximal to a given cell membrane molecule. EMARS analysis identified some BiCAT, such as close homolog of L1 (CHL1), fibroblast growth factor 3 (FGFR3) and $\alpha 2$ integrin, which are commonly expressed in mouse primary lung cancer cells and human lung squamous cell carcinoma cells. Analysis of cancer specimens from 55 lung cancer patients revealed that CHL1 and $\alpha 2$ integrin were highly co-expressed in almost all cancer tissues compared with normal lung tissues. As an example of BiCAT application, *in vitro* simulation of effective drug combinations used for multiple drug treatment strategies was performed using reagents targeted to BiCAT molecules. The combination treatment based on BiCAT information moderately suppressed cancer cell proliferation compared with single administration, suggesting that the information about BiCAT in cancer cells is useful for the appropriate selection of the combination among molecular targeted reagents. Thus, BiCAT has the potential to contribute to several molecular targeted strategies in future.

KEYWORDS

cancer therapy, lipid raft, lung cancer, membrane protein, protein-protein interaction

1 | INTRODUCTION

Molecular targeted strategies using specific targets in cancer cells have been widely used in the field of drug discovery,^{1,2} drug delivery,³ drug administration⁴ and diagnosis.^{5,6} The application of these

treatment strategies has resulted in good outcomes in terms of cancer diagnosis and treatment. However, there are still many difficulties in the development of novel cancer targets that show acceptable efficacy. It is, therefore, necessary to identify novel and potentially effective cancer targets and targeting strategies.

This is an open access article under the terms of the Creative Commons Attribution-NonCommercial License, which permits use, distribution and reproduction in any medium, provided the original work is properly cited and is not used for commercial purposes.

© 2019 The Authors. *Cancer Science* published by John Wiley & Sons Australia, Ltd on behalf of Japanese Cancer Association.

Many molecular targeted strategies have been developed against cell surface (membrane) proteins such as receptor tyrosine kinases (RTK), which are involved in cell proliferation and differentiation. Previous studies have shown that cell surface (membrane) proteins non-randomly form a heterocomplex accompanied by the fluidity of biological membranes.⁷ In particular, regions in the membrane with high concentration of specific molecular complexes together with specific lipids are "lipid rafts." These lipid rafts in the cellular membrane serve as a platform for intracellular signaling and are also involved in various biological phenomena.⁷ In addition, research in drug discovery and treatment against several diseases has focused on lipid rafts.^{3,8,9} Thus, it is essential to identify the molecules that form *cis*-molecular complexes in the cell membrane, especially cancer cell-specific complexes, with the aim of applying these findings to targeted strategies.

Proximity proteomics¹⁰⁻¹³ has recently been used as a method to analyze molecular complexes. We developed a simple and physiological method, called the enzyme-mediated activation of radical source (EMARS) method,¹⁴ which uses HRP-induced radicals derived from arylazide or tyramide compounds.¹⁵ The EMARS radicals attack and form covalent bonds with the proteins in the proximity of the HRP (eg, radicals from arylazide, approximately 200-300 nm,¹⁴ from tyramide, approximately 20 nm¹⁶) because the generated radicals immediately react with surrounding water molecules and disappear when near HRP. Therefore, the bimolecular partner proteins that interact and assemble with an overexpressed given membrane protein, which was selected based on cDNA microarray data, could be labeled only with arylazide or tyramide compounds under physiological conditions (Figures 1 and S1). The labeled proteins can subsequently be analyzed using an antibody array and/or a typical proteome strategy.¹⁷ The EMARS method has been applied in various studies on molecular complexes on the cell membrane.¹⁸⁻²⁴

Here, we propose a "*cis*-bimolecular complex", a biostructure that contains 2 or more different membrane molecules associated with and/or located in close proximity to each other on the same cell membrane, as a new type of cancer target (*cis*-bimolecular cancer target, hereinafter referred to as BiCAT) that was identified in pursuit of diversifying molecular targeted strategies. We used the EMARS method in *Echinoderm Microtubule-associated protein-Like 4-Anaplastic Lymphoma Kinase (EML4-ALK)* transgenic mouse primary lung cancer cells (*EML4-ALK* primary cells) and LK2 human lung squamous cell carcinoma cell line to identify several BiCAT. These BiCAT were also expressed in pathological specimens derived from lung cancer patients.

2 | MATERIALS AND METHODS

Part of the "Materials and Methods" are in Appendix S1.

2.1 | Enzyme-mediated activation of radical source reaction for cell membranes

The EMARS reaction and detection of EMARS products were performed as described previously.¹⁴ Briefly, *EML4-ALK* primary

cells, LK2 cells, HEK293 cells and CHL1 transfectant HEK293 cells were washed once with PBS at room temperature and then treated with either 5 µg/mL of HRP-conjugated anti-mouse CHL1 antibody (AF2147; R&D systems) and anti-human CHL1 antibody (MAB2126; R&D systems) or 4 µg/mL of HRP-conjugated CTxB (LIST Biological Laboratories) in PBS at room temperature for 20 minutes. The cells were then incubated with 0.1 mmol/L fluorescein-conjugated arylazide or fluorescein-conjugated tyramide¹⁵ with 0.0075% H₂O₂ in PBS at room temperature for 15 minutes in the dark. The cell suspension was homogenized through a 26 G syringe needle to break the plasma membranes, and samples were centrifuged at 20 000 g for 15 minutes to precipitate the plasma membrane fractions. After solubilization with NP-40 lysis buffer (20 mmol/L Tris-HCl (pH 7.4), 150 mmol/L NaCl, 5 mmol/L EDTA, 1% NP-40, 1% glycerol), the samples were subjected to SDS-PAGE (10% gel, under non-reducing conditions). Gels were blotted to a PVDF membrane, which was then blocked with 5% skim milk solution. The membranes were then stained with goat anti-fluorescein antibody (Rockland; 0.2 µg/mL) followed by HRP-conjugated anti-goat IgG (1:3000) for FT detection. Alternatively, for the direct detection of fluorescein-labeled proteins in gel, gels after electrophoresis were directly subjected to a ChemiDoc MP Imaging System (BIO-RAD) equipped with filters for fluorescein detection.

2.2 | Staining of pathological specimens from lung cancer patients

This study used a lung cancer patient tissue array (No. OD-CT-RsLug04-003; Shanghai Outdo Biotech) that contains lung carcinoma tissues and normal lung tissues derived from 55 lung cancer patients (30 male and 25 female cases, mongoloid).^{25,26} The specimens were deparaffinized with xylene and 70%-100% ethanol. Antigen retrieval was carried out using L.A.B solution (Polysciences) at room temperature for 10 minutes. The slides were then gently washed with PBS, treated with 5% BSA-PBS for 30 minutes and stained with anti-human CHL1 antibody (4 µg/mL) for 40 minutes followed by Alexa Fluor 546-conjugated anti-rat IgG (Thermo Fisher Scientific) for 40 minutes. After the CHL1 staining, the samples were subsequently stained with anti-α2 integrin antibody (Abcam; ab133557: 4 µg/mL), followed by Alexa Fluor 488-conjugated anti-rabbit IgG (Thermo Fisher Scientific) for 40 minutes. The mounting media containing anti-fade reagent (DABCO; Sigma-Aldrich) and DAPI (Nacalai Tesque) was incubated with specimens before observation. The samples were observed with an LSM 710 Laser Scanning Confocal Microscope (Carl Zeiss) mounted on an AxioImager Z2 equipped with a Diode, argon and He-Ne laser unit. The objective lenses were EC-PLAN NEOFLUAR 5×/0.16 and APOCHROMAT 20×/0.8. Image acquisition and analysis was carried out with ZEN 2011 software (Carl Zeiss). Raw images including differential interference contrast images were captured under identical settings in the experiments and then exported to TIFF files.

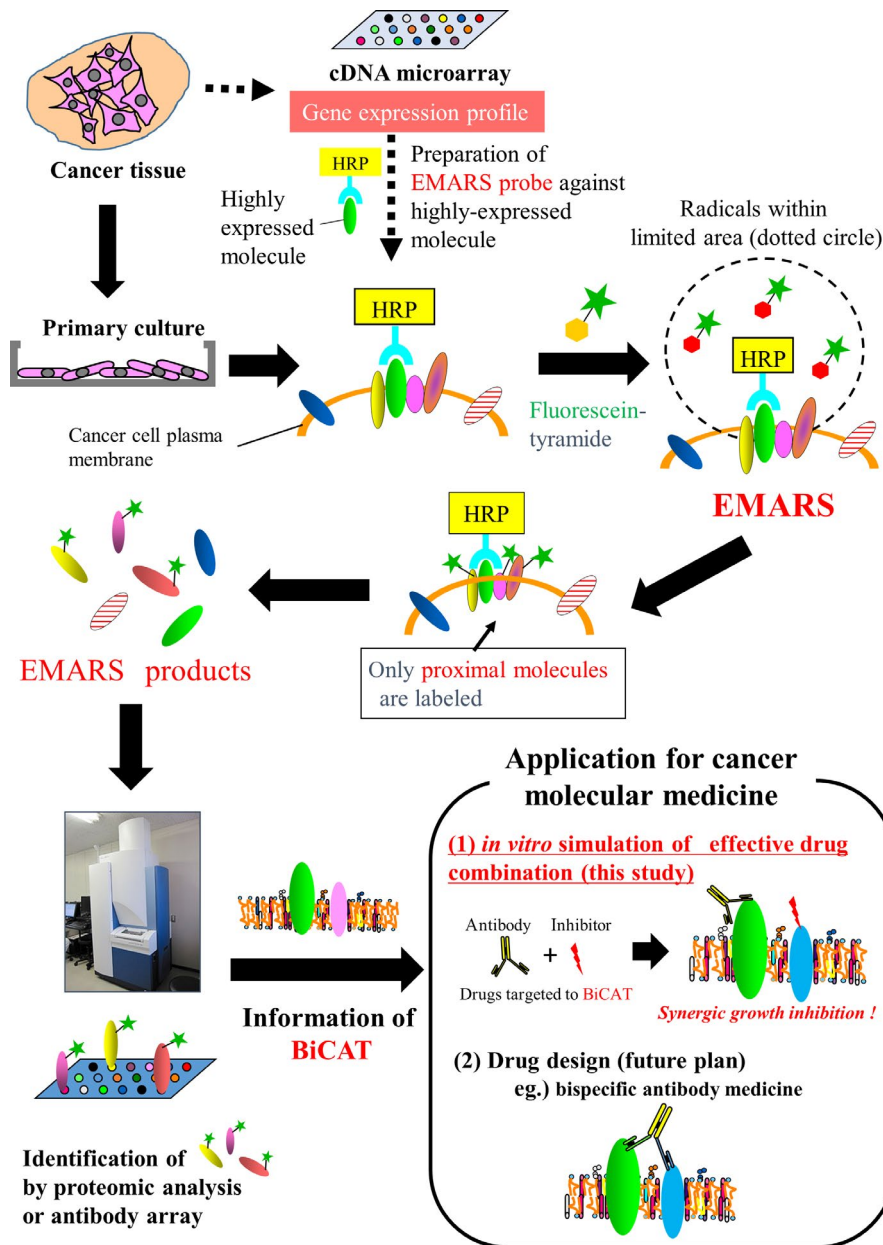


FIGURE 1 Overview of BiCAT analysis for cancer cell membrane. Schematic illustration of BiCAT analysis. Before the enzyme-mediated activation of radical source (EMARS) method, the cancer tissues from *EML4-ALK* transgenic mice were applied to cDNA microarray analysis for the preparation of the EMARS probe, and primary cell inoculation and cultivation. The labeled EMARS products were analyzed using mass spectrometry and/or antibody array

2.3 | In vitro proliferation inhibition assay

EML4-ALK primary cells and LK2 cells were grown on 96-well culture plates (in the case of *EML4-ALK* primary cells, the wells were coated with collagen I). After 72 hours, antibody and/or chemical inhibitors against CHL1, FGFR3 $\alpha 2$ integrin and *EML4-ALK* were added to medium as follows: anti-mouse CHL1 antibody (AF2147; final concentration 2.5 $\mu\text{g}/\text{mL}$), anti-human CHL1 antibody (MAB2126; final concentration 2.5 $\mu\text{g}/\text{mL}$), FGFR inhibitor (PD173074; Cayman Chemical; final concentration 30 nmol/L),²⁷ $\alpha 2\beta 1$ integrin inhibitor (BTT3033; R&D systems; final concentration; 150 nmol/L)^{28,29} and

ALK inhibitor (CH5424802; LKT Laboratories; final concentration; 500 or 1000 nmol/L).³⁰ Although both anti-CHL1 antibodies bind to the extracellular domain of CHL1, the biological effects (ie, an inhibitory or activating effect for CHL1 function) have not been reported. The final concentration of each reagent was determined based on previous reports^{22,27,29} and the data from the pilot studies (data not shown). For the (IgG)₂ antibody³¹⁻³³ preparation, 4 types of antibody mix were prepared by simply mixing with cross-linker antibody as follows: Ab mix 1 (anti-FGFR3 antibody [Santa Cruz; sc-123]: 1 $\mu\text{g}/\text{mL}$ and anti-rabbit IgG Fc specific antibody [Jackson ImmunoResearch; 111-005-046]: 0.5 $\mu\text{g}/\text{mL}$); Ab mix 2 (anti- $\alpha 2$

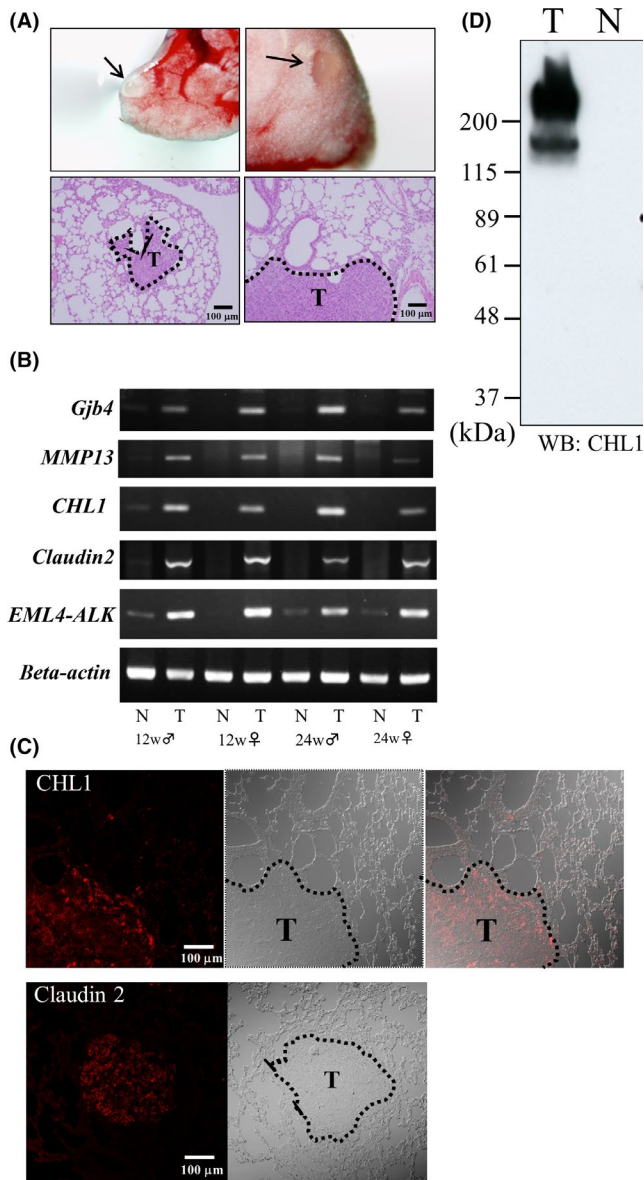


FIGURE 2 CHL1 expression in lung tumors from *EML4-ALK* transgenic mice. **A**, *EML4-ALK* transgenic mouse lung cancers (Arrows). Two representative tumor formations in the lung (upper panel) and HE staining of cancer tissue (lower panel; indicated as the dotted area of "T"). Scale bar: 100 μ m. **B**, RT-PCR analyses of *Gjb4*, *MMP13*, *CHL1*, *Claudin2* and *EML4-ALK* mRNA show potent expression in lung cancer tissue. Tissues derived from 12 and 24-wk old male and female mice were used for the analysis, respectively. N, normal tissue; T, tumor tissue. **C**, Immunohistochemical staining of lung tissues from *EML4-ALK* transgenic mouse. CHL1 staining (upper panel) and Claudin2 staining (lower panel) were performed using anti-CHL1 and anti-Claudin2 antibodies with DIC images. The dotted area indicates the tumor tissue (T). **D**, Protein expression of CHL1 in cancer tissue. Tissue lysate from lung cancer tissue and normal tissue were subjected to western blot analysis using mouse CHL1 antibody. N, normal tissue; T, tumor tissue

integrin antibody [Abcam; ab133557]: 1 μ g/mL and anti-rabbit IgG Fc specific antibody: 0.5 μ g/mL; Ab mix 3 (anti- α 2 integrin antibody: 0.5 μ g/mL, anti- α 2 integrin antibody: 0.5 μ g/mL and anti-rabbit IgG

Fc specific antibody: 0.5 μ g/mL; Ab mix 4 (anti- α 2 integrin antibody: 0.5 μ g/mL, anti- α 2 integrin antibody: 0.5 μ g/mL). These Ab mixes were incubated at room temperature for 30 minutes to form (IgG)₂ antibodies, respectively (Ab mix 3 contains FGFR3- α 2 integrin-(IgG)₂ antibody). After treatment, short-term culture (3-5 days), additional treatment and cell counting were carried out according to 3 protocols: (a) single treatment and cell counting at Day 2 and Day 5; (b) daily treatment and cell counting at Day 2 and Day 4; (c) every-other-day treatment and cell counting at Day 1 and Day 3 with additional treatment at Day 2. Cell counting was performed using the Cell Counting Kit-8 (Dojindo) with a VarioSkan Flash microplate reader (Thermo Scientific) at 450 nm. Each protocol was carried out in multiple independent experiments (a: n = 6, b: n = 5, c: n = 4 [in the case of *EML4-ALK* primary cells: n = 3]). In the case of (IgG)₂ antibody administration, protocol (b) was carried out in multiple independent experiments (n = 4).

3 | RESULTS

3.1 | CHL1 is a suitable molecule for BiCAT analysis in *EML4-ALK* transgenic mice

The overall scheme of BiCAT analysis for cancer cells is summarized in Figure 1. The first step is to identify the overexpressed molecules in cancer cell membranes by cDNA array and prepare the EMARS probe. Next, EMARS is performed in (primary) cancer cells and tissues to identify BiCAT partner molecules associated with overexpressed molecules by proteome analysis. BiCAT information is possibly used for further applications (eg, the simulation of appropriate drug combination for multi-drug administration as described later and drug design).

We used the transgenic mouse of the onco-fusion gene, *EML4-ALK*,^{34,35} which causes spontaneously occurring lung cancer with early onset, since it is suitable for biochemical experiments. We first performed gene expression analysis in both lung tumor and normal tissues from *EML4-ALK* transgenic mice (Figure 2A) by whole mouse cDNA microarray to identify highly expressed membrane molecules in lung tumors (Table S1). We selected 4 genes (*Gjb4*, *MMP13*, *CHL1* and *Claudin 2*) that were overexpressed in lung tumor tissues as candidate membrane proteins. Reverse transcription PCR revealed that these genes were strongly expressed in lung cancer tumors compared with normal tissue (Figure 2B) regardless of sex and age. CHL1 expression was detected in tumor slices (Figure 2C) and in lysates from lung tumors by western blot (Figure 2D), but not in normal lung tissue. CHL1 was reported as an overexpressed gene in human lung carcinoma tissue³⁶ and we thus selected CHL1 for subsequent analysis.

3.2 | Partner molecules constituting BiCAT with CHL1

We next used primary cancer cells derived from lung cancer tissue of *EML4-ALK* transgenic mice (Figure 3A) in EMARS reactions with

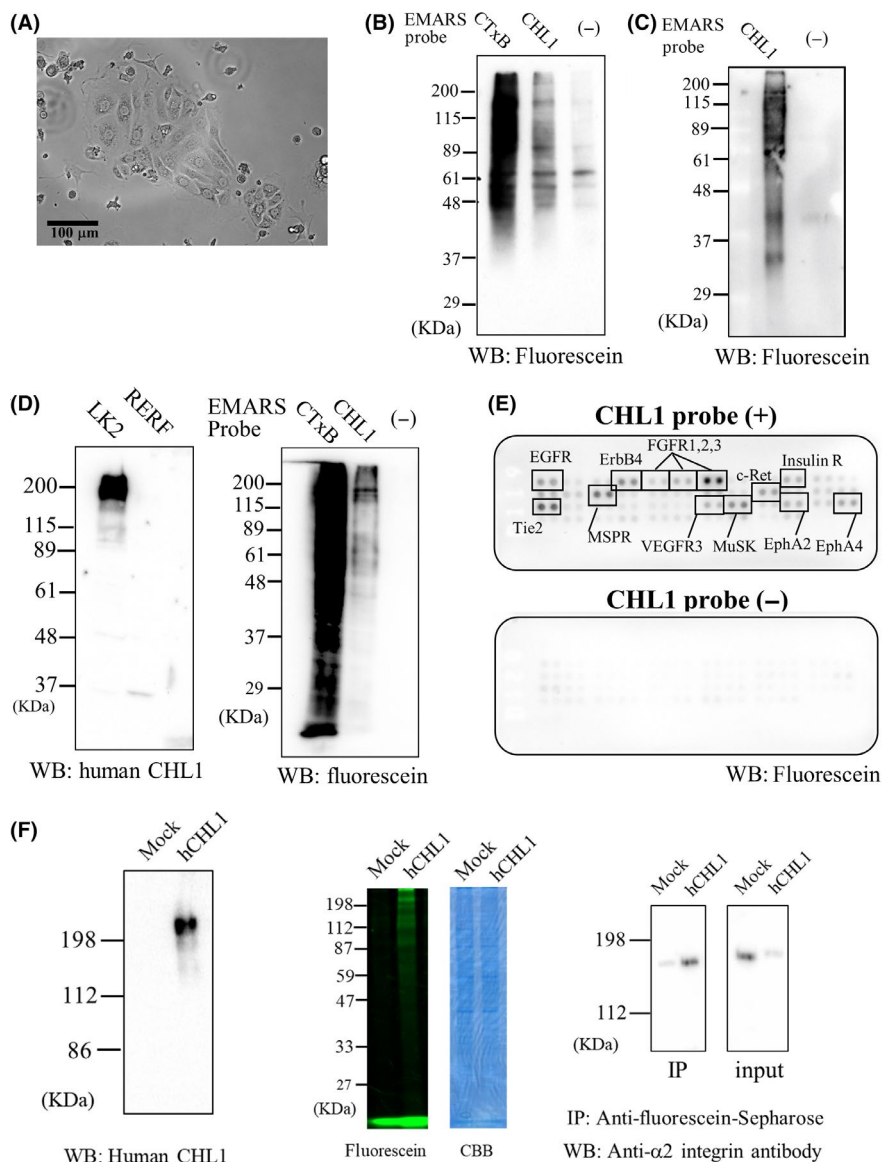


FIGURE 3 BiCAT analysis for cultured cancer cells. A, Representative image of EML4-ALK primary cells. B, C, Partner molecules with CHL1 in EML4-ALK primary cells were labeled with fluorescein-arylazide (B) and fluorescein-tyramide (C) reagent. Enzyme-mediated activation of radical source (EMARS) products were, respectively, subjected to western blot analysis followed by staining using anti-fluorescein antibody. “CTxB” indicates the positive control sample using CTxB probe, “CHL1” the samples using CHL1 probe, and “(-)” the negative control samples (no probe). D, EMARS products labeled with fluorescein-tyramide in LK2 cells. Protein expression level of CHL1 in LK2 and RERF cells (left column). EMARS products by CTxB and human CHL1 probes (right column). Abbreviations are the same as in (C). E, Human receptor tyrosine kinase (RTK) antibody array analysis of EMARS products from LK2 cells. EMARS samples were applied to Human RTK antibody array according to the manufacturer’s instructions. “CHL1 probe (+)” indicates the sample using CHL1 probe, and “CHL1 probe (-)” the negative control samples (no probe). The proteins corresponding to positive RTK were indicated in the array data. F, Interaction between FGFR3 and α 2 integrin in HEK293 cells. HEK293 (mock) and CHL1 transfectant (hCHL1) cells were subjected to western blot analysis with anti-CHL1 antibody (left panel). The EMARS products by HRP-conjugated anti CHL1 antibody from HEK293 and CHL1 transfectant cells were subjected to 10% SDS-PAGE gel followed by direct fluorescein detection (middle panel). Immunoprecipitation experiment of fluorescein-labeled α 2 integrin using anti-fluorescein-Sepharose (right panel). The immunoprecipitation samples and input lysate were subjected to 6% SDS-PAGE gel followed by the western blot analysis with anti- α 2 integrin antibody

CHL1 probes (Figure S2). The CHL1 probes used in this study were HRP-conjugated reduced antibodies recognizing the extracellular domain of human and mouse CHL1. HRP-conjugated cholera toxin subunit B (CTxB probe), which is the cognitive molecule against ganglioside GM1 as a lipid raft marker,³⁷ was used as a positive control.

Using arylazide reagent, the CTxB probe sample generated strong signals; however, moderate signals were observed with the CHL1 probe (Figure 3B). Weak non-specific signals were observed in the negative control sample obtained by EMARS reaction without HRP-conjugated CHL1 probe. In contrast, EMARS reaction using tyramide

reagent showed clear signals in the CHL1 probe sample, with very faint signals in the negative control (Figure 3C), suggesting that tyramide-fluorescein reagent was suitable for this study in terms of specificity and sensitivity.

In the human lung carcinoma cell lines, CHL1 protein was expressed in LK2 cells but not in RERF cells (Figure 3D). EMARS reaction in LK2 cells indicated that both CTxB and human CHL1 probe sample contained fluorescein-labeled proteins, indicated as the partner molecules with CHL1 but not in the negative control sample (Figure 3D). The EMARS products were subsequently used for proteomic analysis with mass spectrometry. The identified membrane (-bound) proteins that are candidates for bimolecular partner molecules with CHL1 are summarized in Table S2 (raw data are in Tables S3–S6). The mass spectrometry analysis is the main tool for BiCAT analysis, but antibody array is also useful in terms of its simplicity and sensitivity, especially for low expression molecules in protein lysates. The human RTK antibody array analysis for LK2 cells demonstrated that EMARS products using CHL1 probe contained some RTK, especially FGFR3 (Figure 3E). We selected 6 membrane (-bound) proteins, $\alpha 2$ integrin, $\beta 1$ integrin, FGFR3, Na/K ATPase, clusterin and contactin1, as bimolecular partners with CHL1.

By using HEK293 cells and its human CHL1 transfectant cells, the interaction between CHL1 and $\alpha 2$ integrin in other cells was examined. HEK293 cells endogenously express $\alpha 2$ integrin, but not CHL1 (Figure 3F, *Left panel*). We performed EMARS reaction in HEK293 cells and CHL1 transfectant cells with HRP-labeled human CHL1 antibody. Several fluorescein-labeled protein bands were observed in CHL1 transfectant HEK293 cells but not in mock cells (Figure 3F, *middle panel*). The immunoprecipitation experiment after EMARS reaction (Figure 3F, *right panel*) revealed that although faint band could be observed in IP sample from mock cells (maybe due to nonspecific binding to Sepharose resin), a clear band was observed in that from CHL1 transfectant cells. It was found that exogenously transfected CHL1 specifically interacts with endogenous $\alpha 2$ integrin in HEK293 cells.

3.3 | Localization of BiCAT in cancer cell membrane

We next examined whether the identified BiCATs co-expressed in the cell membrane. Confocal microscopy showed that $\alpha 2$ integrin (Figure S3A), $\beta 1$ integrin (Figure S3B), clusterin (Figure S3C), Na/K ATPase (Figure S3D), FGFR3 (Figure S3E) and contactin1 (Figure S3F) co-expressed with CHL1, demonstrating that CHL1 and these partner molecules formed BiCAT with each other under an optical microscope. Electron microscopy using LK2 cells (Figure 4A–C) demonstrated that high levels of gold colloid signals of CHL1 (10 nm particles) and partner molecules (5 nm particles) were in proximity on the cell membrane. The proteins were located relatively close to each other, with an interval of approximately 10–50 nm. Moreover, many 5 and 10-nm particles were observed in cellular vesicles (Figure 4A–C), demonstrating that BiCAT existed not only in cell membranes but also in vesicular membranes.

3.4 | BiCAT in pathological specimens from lung cancer patients

Histopathological specimens derived from 55 mongoloid cases of lung cancer patients were stained with antibodies against CHL1 and $\alpha 2$ integrin for the simple detection of representative CHL1 BiCAT identified by our experiments. We first performed analysis under low magnification ($\times 5$ objective) to detect co-expression signals between CHL1 and $\alpha 2$ integrin. CHL1 and the partner molecules were independently expressed in most tissues among 55 cases of lung cancer patients but did not show the same expression patterns among patients (Figure S4). Both whole and local expressions in the sections were observed. Representative imaging of CHL1 and $\alpha 2$ integrin expression is shown in Figure 5A. Some tumor specimens had clear or moderate co-expression signals of CHL1- $\alpha 2$ integrin in the specific areas where cancer cells might be densely packed. The co-expression area of each tumor specimen was then observed under high magnification ($\times 20$ objective) and clear co-expression signals as BiCAT were found in specific cancer cells. Next, we quantified the co-expression area as described in the Supporting Materials and Methods (Appendix S1). By comparison between tumor (Figure 5B) and normal (Figure 5C) tissue slices in each staining, it was found that tumor slices were significantly higher values for CHL1- $\alpha 2$ integrin staining compared with normal slices (4.827 ± 1.562 vs 1.123 ± 0.709 ; $P < 1 \times 10^{-7}$; Figure 5D).

3.5 | In vitro simulation of effective drug combination used for multiple drug treatment strategy based on BiCAT information

Using BiCAT information, we tried a new approach, which was intended for the improvement of multiple drug therapy,³⁸ involving cancer cell proliferation inhibition by multiple antibody/inhibitor administration (anti-CHL1 antibody, FGFR3 inhibitor and $\alpha 2\beta 1$ integrin inhibitor) against the molecules constituting BiCAT. We compared the efficacy between single and double administration of these antibody/inhibitors under 3 administration protocols (every day, once daily and every-other-day protocols; Figures 6A, S5A and S5B). For efficient evaluation of the effects of double administration, the concentration of each agent was set to the appropriate concentration (data not shown). Statistical analyses were performed using both Tukey's test and Dunnett's multiple test (Figure 6B; Dunnett's multiple test). The results of Tukey's analysis are summarized in Table S7.

As shown in Figure S5A, double administration (CHL1 + PD173074, CHL1 + BTT3033 or PD173074 + BTT3033) was moderately effective (approximately 30% average inhibition), in contrast to single administration (approximately 10% average inhibition) for LK2 cells at Day 2. Otherwise, double administration (PD173074 + BTT3033) was only statistically significant for EML4-ALK primary cells at Day 2. The efficacy of double administration at Day 5 seemed to have greater variation or was weaker than that at Day 2 in both cell types. In daily treatments, as shown in Figure 6B, double administration was similarly effective as single treatments, in contrast to no statistically

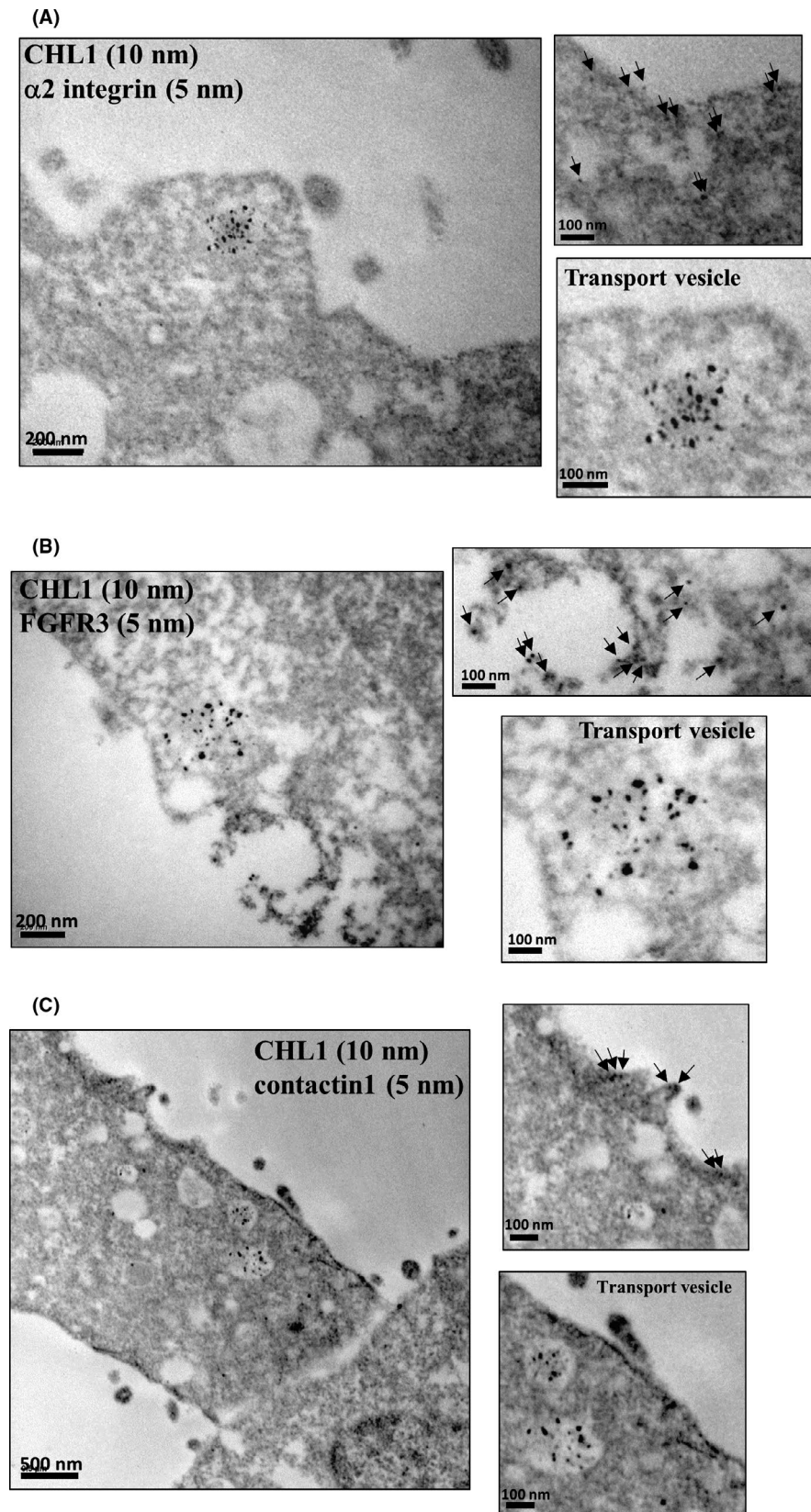


FIGURE 4 BiCAT located in lung cancer cell membranes and cellular vesicles. A-C, Morphological observation of BiCAT in LK2 cells using electron microscopy. Cultured LK2 cells were fixed and co-stained with CHL1 (indicated as 10 nm particles) and partner molecules identified in cell membrane. α 2 integrin (A), FGFR3 (B) and contactin1 (C) were indicated as 5 nm particles. Arrows indicate the locations of gold particles. Scale bar: 100-500 nm

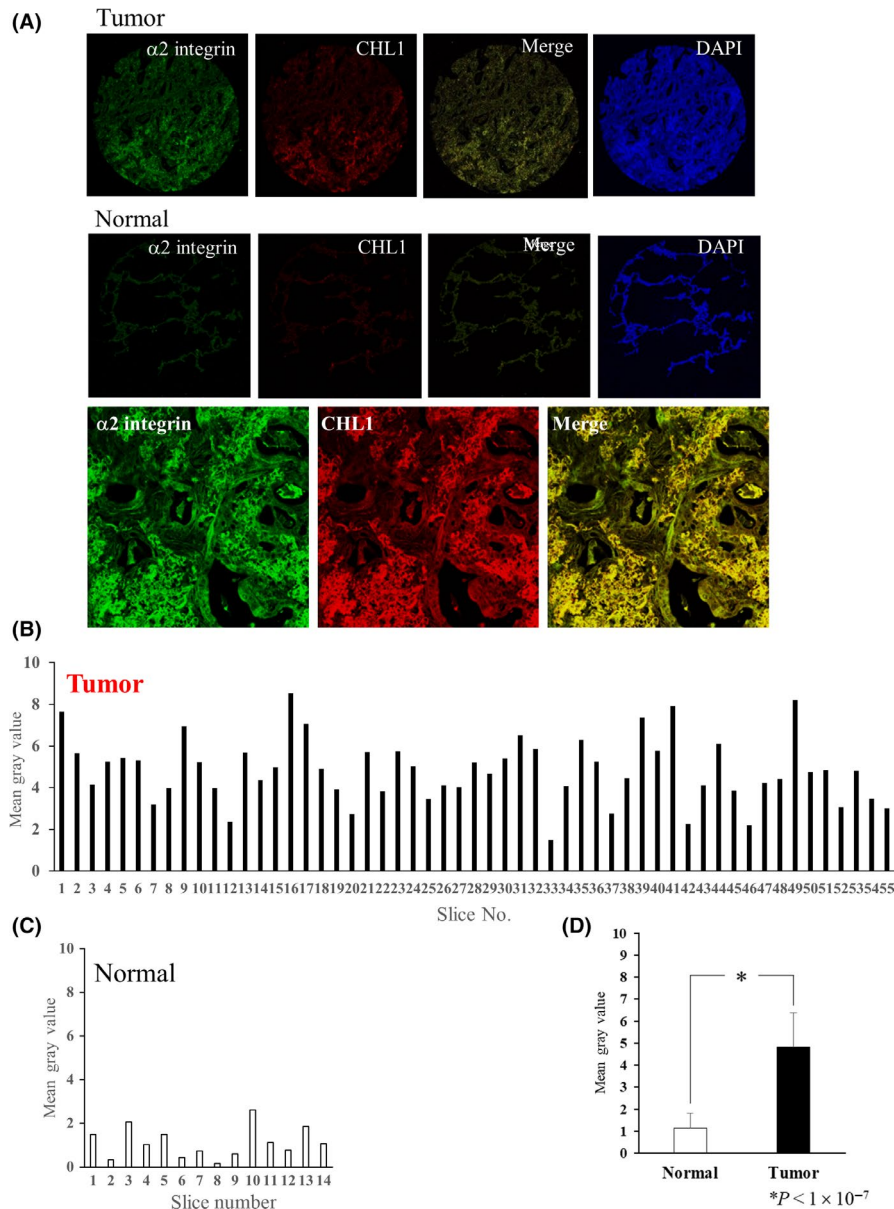


FIGURE 5 BiCAT located in the pathological specimens from lung cancer patients. A, Representative images of CHL1- $\alpha 2$ integrin BiCAT-positive specimens from 55 cases of lung cancer patients. The lung cancer specimens were co-stained with anti-CHL1 antibody (red) and anti- $\alpha 2$ integrin antibody (green), respectively. DAPI solution was used for the nuclear DNA staining. Then, the resulting specimens were observed with confocal microscopy ($\times 5$ objective). Both tumor tissues (upper panel) and normal tissue (middle panel) were stained under the same conditions. Representative images at high magnification observation ($\times 20$ objective; lower panel) in part of the positive region of BiCAT indicated as the merged area (yellow). B, C, Quantitative analysis of co-expression signals of CHL1- $\alpha 2$ integrin BiCAT molecule. The co-expression area was quantified using Image J software as described in the Supporting Materials and Methods (Appendix S1). B, Tumor slices. C, Normal slices. The quantitative values of the co-expression signals are shown in mean gray value. D, Statistical analysis of mean gray value of CHL1- $\alpha 2$ integrin BiCAT between normal and tumor tissues. The analysis was performed with the Mann-Whitney test using R software and EZR. $P < 1 \times 10^{-7}$. The CHL1- $\alpha 2$ integrin BiCAT had significantly higher expression in tumor tissues

significant inhibition after single administration for LK2 cells at Day 2. *EML4-ALK* primary cells at Day 2 showed similar results as cells treated with the single treatment. On Day 4, the double administration was clearly effective for LK2 cells (approximately 50% average inhibition) and moderately effective for *EML4-ALK* primary cells (approximately 30% average inhibition). In the every-other-day treatment condition (Figure S5B), double administration was slightly less

effective than the daily treatment protocol at Day 1 and Day 3 for LK2 cells, except for PD173074 + BTT3033 treatment. For *EML4-ALK* primary cells, double administration showed similar results as those with the daily treatment protocol at Day 1; however, there was significant efficacy in both single and double administration at Day 3. In contrast to these experiments based on BiCAT information, the cell proliferation assay using ALK inhibitors (CH5424802) against

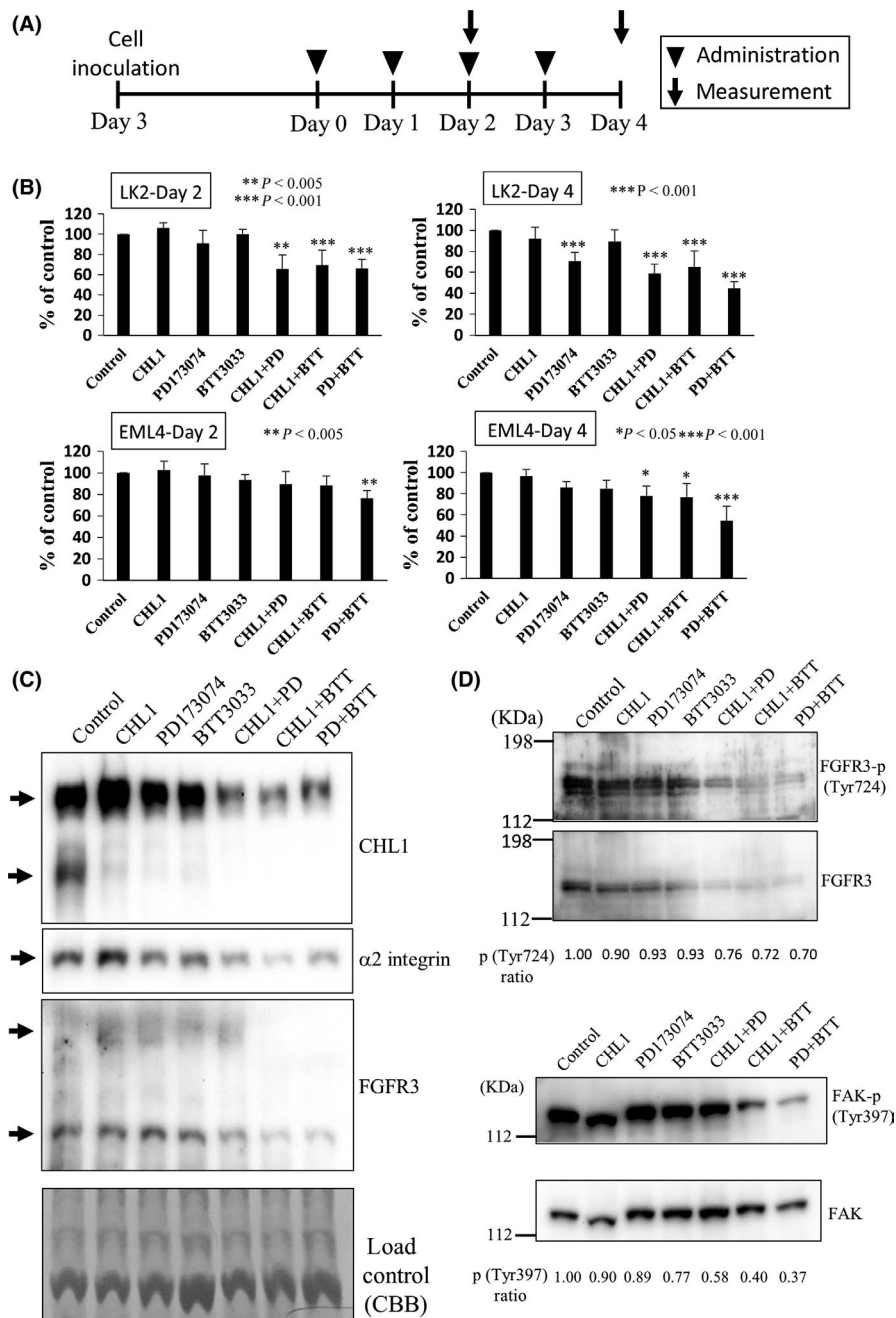


FIGURE 6 In vitro simulation of effective drug combination to inhibit cancer cell proliferation based on BiCAT information. A, The single and double administration under daily treatment protocol ($n = 5$). The administration timing is indicated by closed triangles. The cell numbers of the treated cells were measured on Day 2 and Day 4. B, The relative ratio (% of non-treated cells as control) of cell proliferation rates in LK2 cells and EML4-ALK primary cells. The statistical analysis was performed using Tukey's test and Dunnett's multiple test. The results from Dunnett's test are presented in Figure 6; * $P < 0.05$; ** $P < 0.005$; *** $P < 0.001$. C, Double administration of molecular targeted reagents leads to changes in the expression of partner molecules. The samples of single and double administration under daily treatment conditions (3 d) in LK2 cells were subjected to phos-tag SDS-PAGE and then western blot analysis using CHL1, $\alpha 2$ integrin and FGFR3 antibodies. The CBB staining image indicates load control. The molecular weight markers were not shown in this figure because phos-tag SDS-PAGE cannot show the correct molecular weight of sample proteins. D, Western blot analysis of phosphorylated FGFR3 in single and double administration samples. The samples under daily treatment conditions (3 d) in LK2 cells were subjected to normal SDS-PAGE gel and then western blot analysis using anti-FGFR3 and anti-phospho-FGFR3 antibodies. The quantification of the phosphorylated bands detected in FGFR3 blots was performed using Image J software (ver. 1.51). The ratio of phosphorylation among the samples is indicated below the figure. E, Western blot analysis of phospho-focal adhesion kinase (FAK) in single and double administration samples. The samples under daily treatment conditions (3 d) in LK2 cells were subjected to normal SDS-PAGE and then western blot analysis using anti-FAK and anti-phospho-FAK antibodies

EML4-ALK primary cells showed approximately 10%-30% inhibition at Day 2 and Day 4 (Figure S6).

These experiments under 3 protocols indicated that while the degree of inhibitory ratio differed among the protocols, we observed not only an additive effect but also a synergistic effect for the reagents against BiCAT molecules. For instance, the synergistic inhibitory effects of around 30% were observed at Day 2 with the double administration of 3 reagents in LK2 cells (Figure 6B "LK2-Day 2").

To assess the importance of proximity of BiCAT molecules (FGFR3- α 2 integrin) for cell proliferation inhibition in cancer cells, several (IgG)₂ antibodies³¹⁻³³ (Figure S7A), similar products to bispecific antibodies, were treated with LK2 cells. The binding capacity of each (IgG)₂ antibody was examined using fluorescence microscopy. The patched staining was observed in each sample, suggesting that Ab mix 1-3 contained (IgG)₂ antibodies that induced an antigen crosslinking on the LK2 cell surface (Figure S7B). The Ab mix 1 seemed to bind most strongly to LK2 cells, followed by Ab mix 3 containing FGFR3- α 2 integrin-(IgG)₂ antibody. Although all Ab mixes showed the tendency to inhibit proliferation on Day 4, the treated LK2 cells with Ab mix 3, which theoretically contains FGFR3- α 2 integrin-(IgG)₂ antibody and only one-third of whole (IgG)₂ antibodies, and Ab mix 4 showed statistically significant proliferation inhibition (Figure S7C).

To examine the influence of double treatment, we performed western blot analysis on the reagent treated-cells. The UniProtKB database indicated that human and mouse CHL1, α 2 integrin and FGFR3 are phosphorylated proteins (data not shown). Using Phos-tag gel, CHL1 was detected as 2 bands, which may reflect the differences in phosphorylation of CHL1 (Figure 6C "CHL1"). However, the lower band was only detected in the control sample, so that it is unclear whether double administration affects the phosphorylation in CHL1. In contrast, the upper bands were clearly reduced in only double administration samples (CHL1 + PD173074, CHL1 + BTT3033 or PD173074 + BTT3033) compared with the control and other single administration samples, despite equal amounts of loaded samples. As with CHL1, FGFR3 was detected as 2 bands and was reduced in both CHL1 + BTT3033 and PD173074 + BTT3033 double administration samples (Figure 6C "FGFR3"). To confirm whether phosphorylation in these molecules is changed by double administration, the western blot analysis using normal SDS-PAGE gel was performed and stained with anti-phospho antibody. The slight alterations of phosphorylation in FGFR3 were observed in double administration samples (CHL1 + PD 173074, CHL1 + BTT 3033 or PD 173074 + BTT 3033) (Figure 6D). Unfortunately, in the case of CHL1, the bands of phosphorylated CHL1 could not be detected in all samples by using normal SDS-PAGE gel (data not shown). Although some changes of phosphorylation in FGFR3 were detected in double administration samples, the contribution of phosphorylation was unclear because it was not a critical change. α 2 integrin in the samples with double administration was reduced, whereas there was no significant gel shift of α 2 integrin in the double administration samples (Figure 6C " α 2 integrin"). To investigate whether total integrin functions are affected by double administration, we observed phosphorylation of focal

adhesion kinase (FAK), which is the downstream signal molecule of integrin³⁹ using western blot analysis. The decrease of phosphorylation of FAK was observed in the double administration sample (Figure 6E).

4 | DISCUSSION

Here, we examined whether a BiCAT is useful as a novel cancer target for molecular targeted strategies in terms of improving specificity by designation of 2 or more molecules compared to 1 molecule antigen.⁴⁰

The EMARS method that we previously developed¹⁴ could be suitable for clarifying BiCAT in primary cancer cells under physiological conditions. We selected *EML4-ALK* transgenic mice for the study as the primary culture cells can be relatively easily established from the lung cancer tumor tissue derived from these mice. The establishment of primary culture cells from human cancer tissues has been reported.⁴¹ If primary culture cells can similarly be developed from human cancer biopsy tissue, BiCAT could possibly be simply identified using the EMARS method for each patient, resulting in personalized cancer medicine. Furthermore, the primary cancer cells are important for the in vitro simulation of medicine selection described in Figure 6.

Considering high expression and high specificity cancer antigen is typically required, the selected target molecule for EMARS probe was preferable to be high expression and specificity in cancer tissue. It is, therefore, necessary to perform preliminary experiments (eg, cDNA microarray) or pre-assessment for the determination of appropriate molecules. In the *EML4-ALK* transgenic mouse, CHL1 expression was restricted to the cancer tissue without any correlations to age and sex (Figure 2B), suggesting that CHL1 is a good candidate target molecule. CHL1 is a cell adhesion molecule and has been reported to be involved in several neuronal functions (eg, neurite outgrowth and dendrite orientation in the cerebellar and hippocampal neurons).^{42,43} However, it should be taken into consideration that partner molecules that form BiCAT with CHL1 are highly likely to form BiCAT with each other. In this study, we may also have to consider the combinations among FGFR3, α 2 integrin and contactin1.

In the proteomics analysis of EMARS products with mass spectrometry, there was no overlap of listed candidate molecules between *EML4-ALK* primary cells and LK2 cells (Table S2), indicating that the partner molecules constituting BiCAT with CHL1 were different among cancer cell types or species. However, we hypothesized that the partner molecule information obtained from *EML4-ALK* primary cells was applicable to LK2 cells and vice versa because it is sometimes insufficient to analyze due to differences in the ionization efficiency of molecules in mass spectrometry. Using cDNA microarray data, we also examined the changes of expression levels of representative partner molecules identified above. There was no significant change (data not shown), indicating that BiCAT formation was not simply dependent on the overexpression of both constituent molecules that occurs in cancer.

The immunostaining experiment of lung cancer tissues derived from lung cancer patients provides crucial information for the clinical application of BiCAT. Using quantitative analysis, we found that CHL1- α 2 integrin BiCAT may be expressed in human lung cancer tumor tissue, and almost all tumor slices (92.7%) became "positive" for CHL1- α 2 integrin staining compared to the quantitative data in normal tissues. In lung cancer treatment, epithelial growth factor receptor (EGFR), including its mutant form, and *EML4-ALK* are highly expressed, and are well-known targets for molecular targeted lung cancer drugs such as gefitinib,^{44,45} cetuximab⁴⁶ and crizotinib.⁴⁷ A previous study reported that EGFR is overexpressed in 40%-80% of non-small cell lung cancer patients,⁴⁸ and EGFR mutations have also been detected in 19.4% of lung cancer patients.⁴⁹ The *EML4-ALK* fusion gene was detected in 6.7% of non-small cell lung cancer patients.³⁴ The expression property of CHL1- α 2 integrin BiCAT on the slices is thought to be as good as for typical antigens.

As a new approach to molecular targeted strategy, we attempted to perform a simulation of effective drug combinations for multiple drug administration³⁸ that inhibit cancer cell proliferation based on BiCAT information. This is based on previous findings that molecular complexes are important for signal transduction involved in cell functions through affecting other signals.⁵⁰ For instance, CHL1 and integrins cooperatively contribute to signal transduction by interacting with each other.⁵¹⁻⁵³ Considering this concept, a bispecific antibody may be the best tool to discuss whether the proximity (interaction) among BiCAT molecules is important for cancer cell proliferation inhibition. In this study, we used (IgG)₂ antibodies³¹⁻³³ for the assay because they can be generated in less time than bispecific antibodies. The (IgG)₂ antibodies containing FGFR3- α 2 integrin-(IgG)₂ antibody significantly inhibited cell proliferation in LK2 cells (Figure S7), suggesting that the proximity (interaction) among BiCAT molecules is also an important factor. However, the effect was also observed in the double administration of single FGFR3 and α 2 integrin antibodies, similar to the double administration experiments described in Figure 6B, suggesting that similar cell proliferation inhibition is possibly induced by single antibody combination treatment other than bispecific antibody treatment.

Although our results could not completely demonstrate whether bimolecular interactions in BiCAT contribute to the synergistic action of each reagent, BiCAT information has the potential to help inform drug selection for multiple drug therapy with synergistic effects. The efficacies of double administration in this study were not very powerful (especially for *EML4-ALK* primary cells), and, thus, it seems necessary to improve on the selection of appropriate BiCAT in further studies. The molecular mechanism of this synergistic inhibition based on BiCAT information has never been clearly identified; however, our results suggest that the decreased expression of BiCAT molecules induced by double administration may contribute to synergistic inhibition. In the phosphorylation, significant phosphorylation change was not clearly observed in double administration samples (Figure 6C,D), suggesting that the phosphorylation change in the BiCAT molecule itself may be a partial but not a critical factor of proliferation inhibition. Because each agent inhibits the phosphorylation of the target molecule itself like many molecular targeted

medicines, the mechanism of the cell proliferation inhibitory effect by BiCAT-dependent double administration is of interest. Regarding the decrease in the expression of BiCAT molecules, there is some contribution to the synergistic inhibition, but it is unknown how double administration induces the decrease in the expression of each BiCAT molecule. In contrast, the double administration induced the decrease of FAK signaling in the downstream of integrin (Figure 6E), indicating that the regulation of BiCAT molecules by drug treatment affects not only the expression of BiCAT molecules themselves but also the overall signal transductions and cellular functions.

Moreover, it would be interesting if BiCAT information could contribute to the development of antibody medicine^{32,54} in recognizing cancer-specific BiCA for cancer treatment. In fact, strategies with antibodies recognizing 2 cell membrane molecules have already been developed as molecular targeted bispecific antibody medicine for cancer treatment.^{32,54} Among them, the bispecific antibodies recognizing *cis*-bimolecules similar to BiCAT have only been reported in a few cases (EGFR-IGFR,⁵⁵ EGFR-Met,⁵⁶ CD20-CD22⁵⁷). These anticancer targets are well known and predictable. In our strategy, because of direct identification of proximity molecules on cell membrane, it is an advantage to find not only bimolecules that are predictable based on past findings, but also completely unknown bimolecules that are impossible to predict.

In conclusion, BiCAT have specific features and advantages in terms of the possibility of the development of novel targets and the improvement of antigen specificity not present in typical cancer targets, and may contribute to the discovery of effective and novel molecular targets.

ACKNOWLEDGMENTS

We thank Professor Hiroyuki Mano and Dr Manabu Soda for providing *EML4-ALK* transgenic mice, Professor Tsumoru Shintake for helping with electron microscopic analysis, and the Kochi University experimental training equipment facility and Saitama Medical University Biomedical Research Center for technical assistance. We also thank Edanz Group (www.edanzediting.com/ac) for editing a draft of this manuscript.

DISCLOSURE

The authors declare that they have no conflicts of interest with the contents of this article.

ORCID

Norihiro Kotani  <https://orcid.org/0000-0003-3739-6478>

REFERENCES

1. Terstappen GC, Schlüpen C, Raggiaschi R, Gaviraghi G. Target deconvolution strategies in drug discovery. *Nat Rev Drug Discov*. 2007;6:891-903.

2. Tsuruo T, Naito M, Tomida A, et al. Molecular targeting therapy of cancer: drug resistance, apoptosis and survival signal. *Cancer Sci*. 2003;94:15-21.
3. Rajendran L, Knölker H-J, Simons K. Subcellular targeting strategies for drug design and delivery. *Nat Rev Drug Discov*. 2010;9:29-42.
4. Verweij J, de Jonge M, Eskens F, Sleijfer S. Moving molecular targeted drug therapy towards personalized medicine: issues related to clinical trial design. *Mol Oncol*. 2012;6:196-203.
5. Goldenberg DM, Sharkey RM, Paganelli G, Barbet J, Chatal J-F. Antibody pretargeting advances cancer radioimmunodetection and radioimmunotherapy. *J Clin Oncol*. 2006;24:823-834.
6. Sharkey RM, Karacay H, McBride WJ, Rossi EA, Chang C-H, Goldenberg DM. Bispecific antibody pretargeting of radionuclides for immuno-single-photon emission computed tomography and immuno-positron emission tomography molecular imaging: an update. *Clin Cancer Res*. 2007;13:5577s-5585s.
7. Brown DA, London E. Functions of lipid rafts in biological membranes. *Annu Rev Cell Dev Biol*. 1998;14:111-136.
8. Escribá PV. Membrane-lipid therapy: a new approach in molecular medicine. *Trends Mol Med*. 2006;12:34-43.
9. Mollinedo F, de la Iglesia-Vicente J, Gajate C, et al. Lipid raft-targeted therapy in multiple myeloma. *Oncogene*. 2010;29:3748-3757.
10. Bar DZ, Atkatsk K, Tavarez U, Erdos MR, Gruenbaum Y, Collins FS. Biotinylation by antibody recognition—a method for proximity labeling. *Nat Methods*. 2017;15:127-133.
11. Bar DZ, Atkatsk K, Tavarez U, Erdos MR, Gruenbaum Y, Collins FS. Addendum: biotinylation by antibody recognition—a method for proximity labeling. *Nat Methods*. 2018;15:749.
12. Kim DI, Roux KJ. Filling the void: proximity-based labeling of proteins in living cells. *Trends Cell Biol*. 2016;26:804-817.
13. Rees JS, Li X-W, Perrett S, Lilley KS, Jackson AP. Protein neighbors and proximity proteomics. *Mol Cell Proteomics*. 2015;14:2848-2856.
14. Kotani N, Gu J, Isaji T, Udaka K, Taniguchi N, Honke K. Biochemical visualization of cell surface molecular clustering in living cells. *Proc Natl Acad Sci*. 2008;105:7405-7409.
15. Miyagawa-Yamaguchi A, Kotani N, Honke K. Each GPI-anchored protein species forms a specific lipid raft depending on its GPI attachment signal. *Glycoconj J*. 2015;32:531-540.
16. Sato S, Hatano K, Tsushima M, Nakamura H. 1-Methyl-4-aryl-urazole (MAUra) labels tyrosine in proximity to ruthenium photocatalysts. *Chem Commun (Camb)*. 2018;54:5871-5874.
17. Jiang S, Kotani N, Ohnishi T, et al. A proteomics approach to the cell-surface interactome using the enzyme-mediated activation of radical sources reaction. *Proteomics*. 2012;12:54-62.
18. Hashimoto N, Hamamura K, Kotani N, et al. Proteomic analysis of ganglioside-associated membrane molecules: substantial basis for molecular clustering. *Proteomics*. 2012;12:3154-3163.
19. Ishiura Y, Kotani N, Yamashita R, Yamamoto H, Kozutsumi Y, Honke K. Anomalous expression of Thy1 (CD90) in B-cell lymphoma cells and proliferation inhibition by anti-Thy1 antibody treatment. *Biochem Biophys Res Commun*. 2010;396:329-334.
20. Iwamaru Y, Kitani H, Okada H, et al. Proximity of SCG10 and prion protein in membrane rafts. *J Neurochem*. 2016;136:1204-1218.
21. Kaneko K, Ohkawa Y, Hashimoto N, et al. Neogenin, defined as a GD3-associated molecule by enzyme-mediated activation of radical sources, confers malignant properties via intracytoplasmic domain in melanoma cells. *J Biol Chem*. 2016;291:16630-16643.
22. Kotani N, Ishiura Y, Yamashita R, Ohnishi T, Honke K. Fibroblast growth factor receptor 3 (FGFR3) associated with the CD20 antigen regulates the rituximab-induced proliferation inhibition in B-cell lymphoma cells. *J Biol Chem*. 2012;287(44):37109-37118.
23. Ohkawa Y, Momota H, Kato A, et al. Ganglioside GD3 enhances invasiveness of gliomas by forming a complex with platelet-derived growth factor receptor α and yes kinase. *J Biol Chem*. 2015;290:16043-16058.
24. Yamashita R, Kotani N, Ishiura Y, Higashiyama S, Honke K. Spatiotemporally-regulated interaction between β 1 integrin and ErbB4 that is involved in fibronectin-dependent cell migration. *J Biochem*. 2011;149:347-355.
25. Gao X, Feng J, He Y, et al. hnRNPK inhibits GSK3 β Ser9 phosphorylation, thereby stabilizing c-FLIP and contributes to TRAIL resistance in H1299 lung adenocarcinoma cells. *Sci Rep*. 2016;6:22999.
26. Zhao Q. RNAi-mediated silencing of praline-rich gene causes growth reduction in human lung cancer cells. *Int J Clin Exp Pathol*. 2015;8:1760-1767.
27. Mohammadi M, Froum S, Hamby JM, et al. Crystal structure of an angiogenesis inhibitor bound to the FGF receptor tyrosine kinase domain. *EMBO J*. 1998;17:5896-5904.
28. Miller MW, Basra S, Kulp DW, et al. Small-molecule inhibitors of integrin α 2 β 1 that prevent pathological thrombus formation via an allosteric mechanism. *Proc Natl Acad Sci USA*. 2009;106:719-724.
29. Nissinen L, Ojala M, Langen B, et al. Sulfonamide inhibitors of α 2 β 1 integrin reveal the essential role of collagen receptors in in vivo models of inflammation. *Pharmacol Res Perspect*. 2015;3:e00146.
30. Sakamoto H, Tsukaguchi T, Hiroshima S, et al. CH5424802, a selective ALK inhibitor capable of blocking the resistant gatekeeper mutant. *Cancer Cell*. 2011;19:679-690.
31. Patterson JT, Gros E, Zhou H, et al. Chemically generated IgG2 bispecific antibodies through disulfide bridging. *Bioorg Med Chem Lett*. 2017;27:3647-3652.
32. Kontermann R. Dual targeting strategies with bispecific antibodies. *MAbs*. 2012;4:182-197.
33. Müller D, Kontermann RE. Bispecific antibodies for cancer immunotherapy: current perspectives. *BioDrugs*. 2010;24:89-98.
34. Soda M, Choi YL, Enomoto M, et al. Identification of the transforming EML4-ALK fusion gene in non-small-cell lung cancer. *Nature*. 2007;448:561-566.
35. Soda M, Takada S, Takeuchi K, et al. A mouse model for EML4-ALK-positive lung cancer. *Proc Natl Acad Sci*. 2008;105:19893-19897.
36. Senchenko VN, Krasnov GS, Dmitriev AA, et al. Differential expression of CHL1 gene during development of major human cancers. Creighton C, ed. *PLoS ONE*. 2011;6:e15612.
37. Aureli M, Mauri L, Ciampa MG, et al. GM1 ganglioside: past studies and future potential. *Mol Neurobiol*. 2016;53:1824-1842.
38. Li F, Zhao C, Wang L. Molecular-targeted agents combination therapy for cancer: developments and potentials. *Int J Cancer*. 2014;134:1257-1269.
39. Mitra SK, Schlaepfer DD. Integrin-regulated FAK-Src signaling in normal and cancer cells. *Curr Opin Cell Biol*. 2006;18:516-523.
40. Intlekofer AM, Younes A. Precision therapy for lymphoma—current state and future directions. *Nat Rev Clin Oncol*. 2014;11:585-596.
41. Mitra A, Mishra L, Li S. Technologies for deriving primary tumor cells for use in personalized cancer therapy. *Trends Biotechnol*. 2013;31:347-354.
42. Demyanenko GP, Schachner M, Anton E, et al. Close homolog of L1 modulates area-specific neuronal positioning and dendrite orientation in the cerebral cortex. *Neuron*. 2004;44:423-437.
43. Hillenbrand R, Molthagen M, Montag D, Schachner M. The close homologue of the neural adhesion molecule L1 (CHL1): patterns of expression and promotion of neurite outgrowth by heterophilic interactions. *Eur J Neurosci*. 1999;11:813-826.
44. Lynch TJ, Bell DW, Sordella R, et al. Activating mutations in the epidermal growth factor receptor underlying responsiveness of non-small-cell lung cancer to gefitinib. *N Engl J Med*. 2004;350:2129-2139.
45. Paez JG, Jänne PA, Lee JC, et al. EGFR mutations in lung cancer: correlation with clinical response to gefitinib therapy. *Science*. 2004;304:1497-1500.

46. Kawamoto T, Sato JD, Le A, Polikoff J, Sato GH, Mendelsohn J. Growth stimulation of A431 cells by epidermal growth factor: identification of high-affinity receptors for epidermal growth factor by an anti-receptor monoclonal antibody. *Proc Natl Acad Sci USA*. 1983;80:1337-1341.
47. Choi YL, Soda M, Yamashita Y, et al. EML4-ALK mutations in lung cancer that confer resistance to ALK inhibitors. *N Engl J Med*. 2010;363:1734-1739.
48. Arteaga CL. ErbB-targeted therapeutic approaches in human cancer. *Exp Cell Res*. 2003;284:122-130.
49. Mitsudomi T, Yatabe Y. Mutations of the epidermal growth factor receptor gene and related genes as determinants of epidermal growth factor receptor tyrosine kinase inhibitors sensitivity in lung cancer. *Cancer Sci*. 2007;98:1817-1824.
50. Simons K, Toomre D. Lipid rafts and signal transduction. *Nat Rev Mol Cell Biol*. 2000;1:31-39.
51. Buhusi M, Midkiff BR, Gates AM, Richter M, Schachner M, Maness PF. Close homolog of L1 is an enhancer of integrin-mediated cell migration. *J Biol Chem*. 2003;278:25024-25031.
52. Katic J, Loers G, Kleene R, et al. Interaction of the cell adhesion molecule CHL1 with vitronectin, integrins, and the plasminogen activator inhibitor-2 promotes CHL1-induced neurite outgrowth and neuronal migration. *J Neurosci*. 2014;34:14606-14623.
53. Maness PF, Schachner M. Neural recognition molecules of the immunoglobulin superfamily: signaling transducers of axon guidance and neuronal migration. *Nat Neurosci*. 2007;10:19-26.
54. Byrne H, Conroy PJ, Whisstock JC, O'Kennedy RJ. A tale of two specificities: bispecific antibodies for therapeutic and diagnostic applications. *Trends Biotechnol*. 2013;31:621-632.
55. Lu D, Zhang H, Ludwig D, et al. Simultaneous blockade of both the epidermal growth factor receptor and the insulin-like growth factor receptor signaling pathways in cancer cells with a fully human recombinant bispecific antibody. *J Biol Chem*. 2004;279:2856-2865.
56. Castoldi R, Ecker V, Wiehle L, et al. A novel bispecific EGFR/Met antibody blocks tumor-promoting phenotypic effects induced by resistance to EGFR inhibition and has potent antitumor activity. *Oncogene*. 2013;32:5593-5601.
57. Rossi EA, Goldenberg DM, Cardillo TM, Stein R, Chang C-H. Hexavalent bispecific antibodies represent a new class of anticancer therapeutics: 1. Properties of anti-CD20/CD22 antibodies in lymphoma. *Blood*. 2009;113:6161-6171.

SUPPORTING INFORMATION

Additional supporting information may be found online in the Supporting Information section at the end of the article.

How to cite this article: Kotani N, Yamaguchi A, Ohnishi T, et al. Proximity proteomics identifies cancer cell membrane cis-molecular complex as a potential cancer target. *Cancer Sci*. 2019;110:2607-2619. <https://doi.org/10.1111/cas.14108>